


Article

Vegetative Insecticidal Protein Vip3Aa Is Transported via Membrane Vesicles in *Bacillus thuringiensis* BMB171

Yizhuo Zhang ¹, Xuelian Li ¹, Hongwei Tian ¹, Baoju An ¹, Bing Yan ¹ and Jun Cai ^{1,2,3,*} 

¹ Department of Microbiology, College of Life Sciences, Nankai University, Tianjin 300071, China; 2120201040@mail.nankai.edu.cn (Y.Z.); 2120201043@mail.nankai.edu.cn (X.L.); 2120211166@mail.nankai.edu.cn (H.T.); 1120190491@mail.nankai.edu.cn (B.A.); iceyan@nankai.edu.cn (B.Y.)

² Key Laboratory of Molecular Microbiology and Technology, Ministry of Education, Tianjin 300071, China

³ Tianjin Key Laboratory of Microbial Functional Genomics, Tianjin 300071, China

* Correspondence: caijun@nankai.edu.cn

Abstract: Vegetative insecticidal protein Vip3Aa, secreted by many *Bacillus thuringiensis* (Bt) strains during the vegetative growth stage, represents the second-generation insecticidal toxin. In recent years, significant progress has been made on its structure and action mechanism. However, how it is translocated across the cytoplasmic membrane into the environment remains a mystery. This work demonstrates that Vip3Aa is not secreted by the General Secretion (Sec) System. To reveal the secretory pathway of Vip3A, we purified the membrane vesicles (MVs) of *B. thuringiensis* BMB171 and observed by TEM. The size of MVs was determined by the dynamic light scattering method, and their diameter was approximately 40–200 nm, which is consistent with the vesicles in Gram-negative bacteria. Moreover, Vip3A could be detected in the purified MVs by Western blot, and immunoelectron microscopy reveals Vip3A antibody-coated gold particles located in the MVs. After deleting its signal peptide, chitinase B (ChiB) failed to be secreted. However, the recombinant ChiB, whose signal peptide was substituted with the N-terminal 39 amino acids from Vip3A, was secreted successfully through MVs. Thus, this sequence is proposed as the signal region responsible for vesicle transport. Together, our results revealed for the first time that Vip3Aa is transported to the medium via MVs.

Keywords: *Bacillus thuringiensis*; Vip3Aa; membrane vesicles; protein secretion

Key Contribution: Here, we purified the membrane vesicles of *B. thuringiensis* BMB171 and found for the first time that the MV pathway can secrete Vip3A. Our study provides a new idea for the application of efficient transport proteins.



Citation: Zhang, Y.; Li, X.; Tian, H.; An, B.; Yan, B.; Cai, J. Vegetative Insecticidal Protein Vip3Aa Is Transported via Membrane Vesicles in *Bacillus thuringiensis* BMB171. *Toxins* **2022**, *14*, 480. <https://doi.org/10.3390/toxins14070480>

Received: 10 June 2022

Accepted: 11 July 2022

Published: 13 July 2022

Publisher's Note: MDPI stays neutral with regard to jurisdictional claims in published maps and institutional affiliations.



Copyright: © 2022 by the authors. Licensee MDPI, Basel, Switzerland. This article is an open access article distributed under the terms and conditions of the Creative Commons Attribution (CC BY) license (<https://creativecommons.org/licenses/by/4.0/>).

1. Introduction

Vegetative insecticidal protein Vip3Aa, secreted by many *Bacillus thuringiensis* (Bt) strains during the vegetative growth stage, shares no sequence and structural homology with known insecticidal crystal proteins (ICPs) [1,2] and represents the second-generation insecticidal toxin. Vip3Aa has broad-spectrum insecticidal activity and a unique mechanism for killing insects [2], which has an excellent control effect on *Spodoptera frugiperda* and other insect pests, such as *Spodoptera exigua*, *Helicoverpa armigera*, *Helicoverpa zea*, *Heliothis virescens*, and *Agrotis ipsilon* [3,4]. More critically, Vip3A shows synergy with some crystal proteins, and no cross-resistance has been observed between these two kinds of proteins so far [5,6]. Consequently, based on the gene-pyramiding strategy, the *vip3A* and the *cry* genes are utilized simultaneously in rice, cotton, and maize for higher efficacy and to delay insect resistance development [7,8].

Vip3A-related research has mainly focused on its architecture and the action mechanism in recent years. The cryo-EM structure reveals that Vip3A is composed of five domains and its molecular architecture is distinctly different from a 3-domains structure

of Cry protein [9,10]. This confirms the previous speculation that Cry and Vip3A toxins do not share receptors in the insect midgut due to structural differences [2]. Moreover, the trypsin-activated structure unravels significant conformational changes upon protease digestion in the N-terminal region [10,11], resulting in the reorganization of domain I into a long needle structure of 200 Å, which remains associated with the rest of the protein. A spring-loaded mechanism was proposed to explain its activation process [10].

Binding to the receptor is a crucial step in the virulence process of Vip3A. Recently, several Vip3A receptors have been identified, including ribosome S2 protein from sf21 cells of *S. frugiperda* [12], scavenger receptor class C protein (Sf-SR-C) [13], fibroblast growth factor receptor protein (Sf-FGFR) [14] and prohibitin 2 (PHB2) from the Sf9 cell lines of *S. frugiperda* [15], and a tenascin-like glycoprotein from *A. ipsilon* [16]. After binding to its receptor, Vip3A may exert its potency through pore formation and induce apoptosis [1,17,18]. Although the pore formation model is most acceptable for the activity of Vip3Aa, more and more evidence shows that the induction of apoptosis through an intrinsic mitochondrial pathway may also be involved in its toxicity [19].

Vip3A was first identified as a secreted protein in the supernatant of *Bt* strain AB88 [20]. By sequence alignment, it was found that the N-terminus of Vip3 is highly conserved. However, Vip3A is not N-terminally processed during export, and sequence analysis using SignalP 6.0 (<https://services.healthtech.dtu.dk/service.php?SignalP-6.0>, accessed on 5 March 2022) reveals that Vip3Aa lacks a classical signal peptide, it is proposed to be secreted through a non-classical secretion pathway. In recent years, significant progress has been made in the structure and mechanism of action of Vip3A, but its secretory mechanism is still undefined. How it translocates across the cytoplasmic membrane remains a mystery.

In this study, we tried to reveal the secretory pathway of Vip3A and define the region responsible for its transport process. We demonstrated that Vip3A is not secreted by General Secretion (Sec) System. Instead, it transports to the medium via membrane vesicles. Furthermore, the N-terminal 39 amino acid sequence of Vip3Aa is proposed as the signal region responsible for vesicle transport, leading ChiB without signal peptides to be secreted by vesicles. These results solve a long-standing question concerning the secretion of the Vip3A, which can improve the secretion of Vip3A and may apply to other proteins.

2. Results

2.1. Vip3A Is Not Secreted via the Sec Secretion Pathway

The ChiB of *Bacillus cereus* is secreted by the Sec system [21]. *B. cereus* and *B. thuringiensis* are closely related bacteria of the *B. cereus* group. Previous research in our laboratory indicated that ChiB from *B. thuringiensis* has a predicted Sec signal peptide and translocates by the Sec system (data not shown). To determine whether Vip3Aa is secreted through the Sec pathway, we preliminarily explored the effect of using the Sec pathway signal peptide of ChiB on Vip3Aa secretion efficiency. To express a large amount of Vip3A protein to determine its secretion, we constructed plasmid pPCspvip3. P_{rsi} is a strong constitutive promoter previously found in our laboratory, and we used it to drive Vip3A expression. Moreover, we used the signal peptide of ChiB to direct the secretion of Vip3A, and Vip3A was detected using an anti-Vip3A antibody. The result showed that although spChiB-Vip3A emerged in the supernatants, contrary to Vip3Aa, much of them have been degraded (Figure 1a). This suggested that when Vip3A secretes through the Sec pathway, it encounters specific proteases that have not been met before. In other words, the ChiB signal peptide transports Vip3A to the culture through a completely different secretory pathway from Vip3A itself.

Additionally, we enhanced the Sec secretion system through overexpression of *secYEG*, which serves as a translocation channel in the Sec secretion system. Under the control of a strong promoter P_{rsi} , a DNA fragment coding for SecYEG-fused protein was integrated onto the BMB171 genome to generate a knock-in strain BMB171-Sec (Figure 1b). We validated the overexpression of *secYEG* by qRT-PCR (Figure 1c).

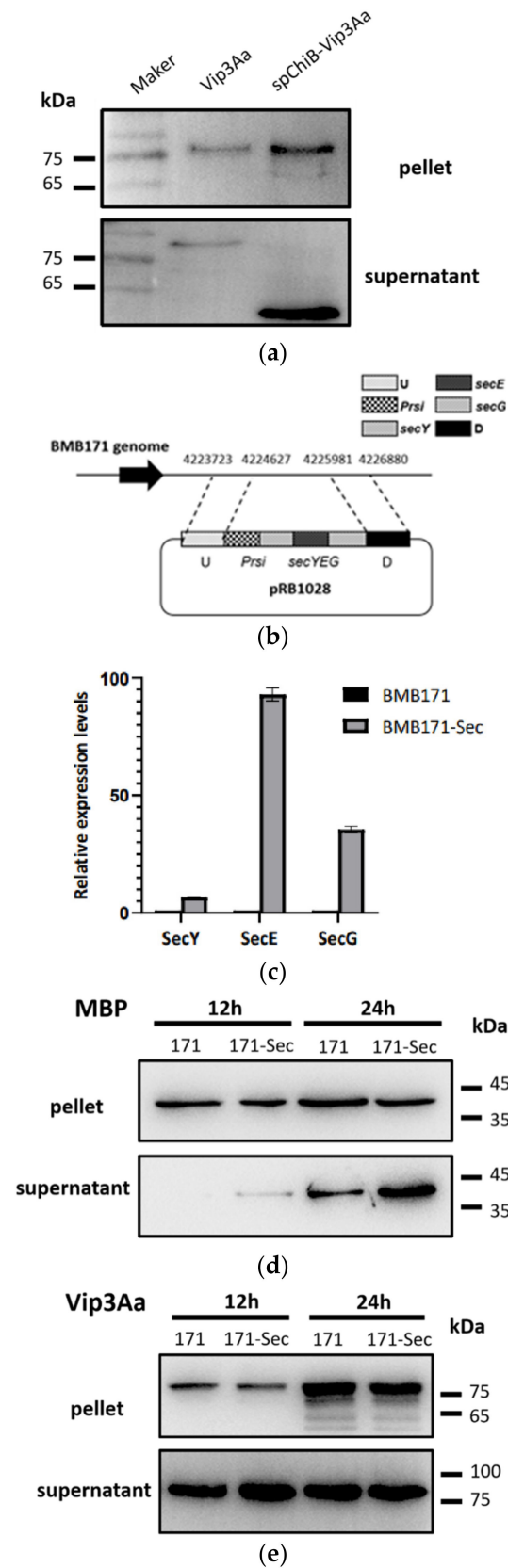


Figure 1. Vip3Aa protein is not secreted via the sec secretion pathway. **(a)** Western blot analysis of Vip3Aa and ChiB signal peptide-guided Vip3Aa in the pellet (upper panel) and the supernatant (lower panel) of BMB171. **(b)** Illustration of how SecYEG-fused protein gene integrated onto the genome of BMB171 strain to generate a knock-in strain BMB171-Sec. **(c)** Relative expression levels of

SecYEG genes in the BMB171 and BMB171-Sec were determined by qRT-PCR analysis. (d,e) Western blot analysis of Maltose Binding Protein (MBP) (d) and Vip3Aa (e) in BMB171 and BMB171-Sec expressed in the pellet (upper panel) and the supernatant (lower panel).

ChiB has high secretion efficiency and few intracellular residues in *B. thuringiensis* BMB 171, which is not conducive to verifying the enhancement of the Sec secretion system. In contrast, the secretion efficiency of Maltose Binding Protein (MBP), a classical Sec system secreted protein derived from *Escherichia coli* K-12, is moderate in *B. thuringiensis* BMB 171. We used it to identify whether Sec-dependent protein secretion efficiency has improved. The recombinant plasmid pHT1K-*vip3A* and pHT1K-*mbp* were transformed into the knock-in strain BMB171-Sec, respectively. The results indicated that the secretion efficiency of MBP enhanced significantly in BMB171-Sec (Figure 1d), while the Vip3A content was similar in the supernatant of BMB171 and BMB171-Sec (Figure 1e). This also supported that the Sec system does not secrete Vip3A.

2.2. Isolation of Vesicles from *B. thuringiensis* BMB171 Culture Supernatants

To investigate whether *B. thuringiensis* produces MVs, we collected vesicles in culture supernatants by hypercentrifugation. After negative staining, some cup-shaped structures with a transparent membrane were visualized using a transmission electron microscope (TEM) (Figure 2a), which is similar to the extracellular vesicles figure from Shao 's review in 2018 [21].

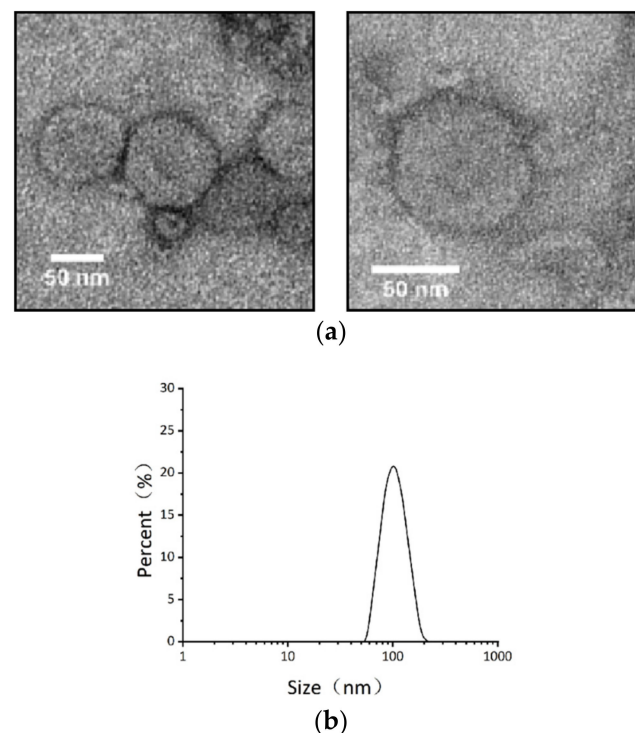


Figure 2. Gram-positive bacteria *B. thuringiensis* BMB171 can produce MVs. (a) Negative-staining TEM of purified MVs (scale bars, 50 nm). (b) Size distribution of MVs measured with dynamic light scattering (DLS) shows the diameter range of 40–200 nm.

Dynamic light scattering analysis showed that the diameter of purified MV ranges from 40 to 200 nm (Figure 2b), consistent with that of Gram-negative bacteria outer membrane vesicles.

2.3. Vip3Aa Were Detected in Membrane Vesicles

Vip3Aa can be detected in vesicles purified from the BMB171/ pHT1K-*vip3A* strain by Western blot analysis (Figure 3a). To determine whether Vip3A is present in the vesicles, we performed immunogold electron microscopy (IEM) of purified vesicles (Figure 3b). The result indicated the presence of Vip3A antibody-coated gold particles in purified vesicles, while immunogold labeling with an antibody against ChiB did not reveal gold particles in isolated vesicles.

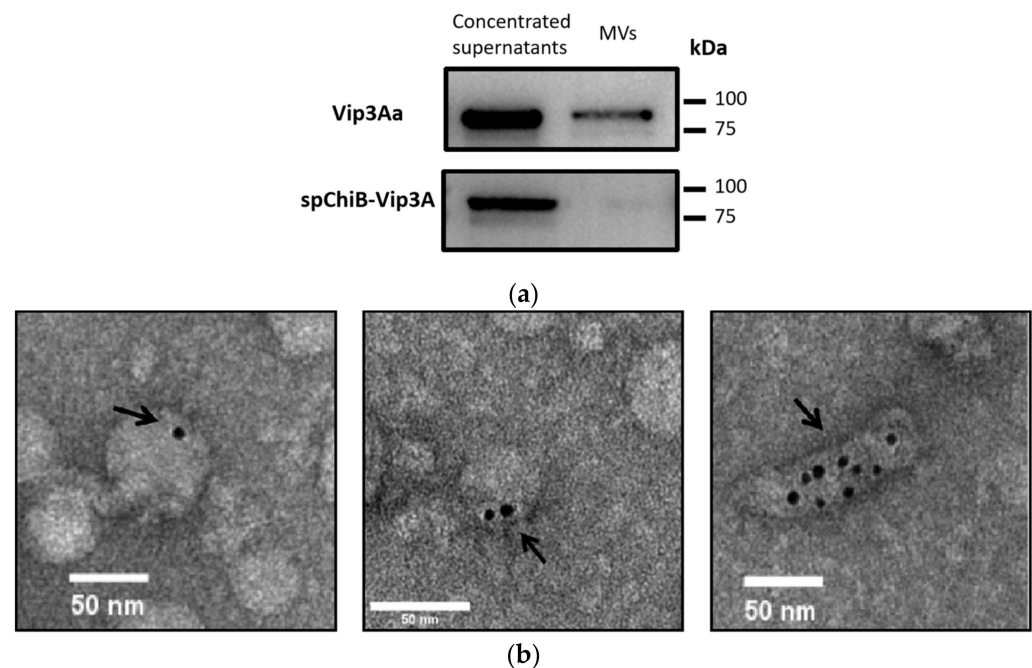


Figure 3. Vip3Aa was detected in membrane vesicles. (a) MVs collected from the culture media of BMB171/Vip3Aa and BMB171/ChiBsp-Vip3Aa were analyzed by Western Blot. Samples were detected by anti-Vip3Aa antibody. (b) Immunoelectron microscopy revealed Vip3Aa in isolated vesicles. Solid arrows, gold particles (6 nm) depicting Vip3Aa binding (scale bars, 50 nm). After permeabilization, some membrane vesicles structure are disrupted and other morphologies appear.

Additionally, vesicles from the BMB171 in which Vip3A is guided by ChiB signal peptide were also collected. We detected Vip3A in the supernatant but not in purified MVs (Figure 3a). This provided further evidence that the ChiB signal peptide-guided Vip3A protein secretion is distinct from Vip3A.

2.4. Vip3Aa α -Helix Plays an Essential Role in Vip3Aa Secretion

The highly conserved N-terminal region of Vip3A was supposed to be responsible for its translocation and virulence. Zack et al. considered that Vip3A contains a putative signal peptide cleavage site at 12ALPSF [22]. However, using deletion mutagenesis to excise amino acid residues 1–11 of the Vip3Aa, we found that the generated mutant protein can still be secreted into the culture supernatant (Figure 4a).

Proteomics of *B. anthracis* MVs identified thirty-six different proteins [23]. When performing the motif analysis by MEME (<http://meme.nbcr.net>, accessed on 3 March 2022), we found no conserved sequence among these proteins and Vip3Aa. However, they have similar characteristics in protein secondary structure. The 3D structure of Vip3Aa shows that its N-terminal contains four helices [10]. Similarly, the protein secondary structure predictions indicated that the N-terminus of *B. anthracis* MV proteins had two or more α -helices. (Figure 4b).

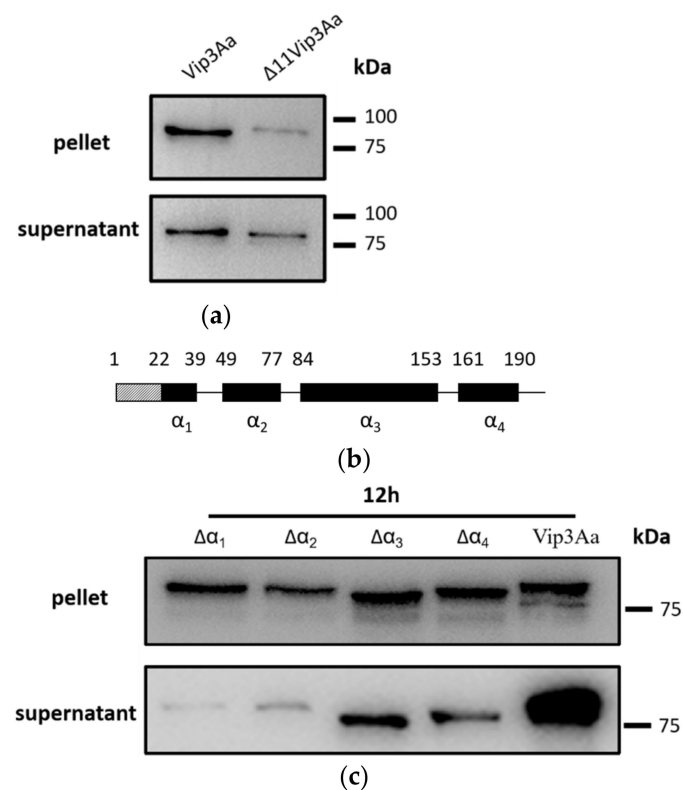


Figure 4. Critical regions of Vip3Aa that affect its secretion. (a) Western blot analysis of Vip3Aa and $\Delta 11$ Vip3Aa expressed in the pellet (upper panel) and the supernatant (lower panel). (b) The organization of Vip3Aa Domain I. (c) Western blot analysis of $\Delta\alpha_1$ -Vip3Aa, $\Delta\alpha_2$ -Vip3Aa, $\Delta\alpha_3$ -Vip3Aa, $\Delta\alpha_4$ -Vip3Aa, and Vip3Aa expressed in different α -helix-deficient strains was visualized in the pellet (upper panel) and the supernatant (lower panel). Samples were collected at 12 h (left) and 24 h (right).

To clarify the effect of these α -helices on the secretion of Vip3Aa, we constructed different α -helix-deficient strains. We found that no matter which α -helix was deleted, Vip3Aa can still be detected in the supernatant (Figure 4c). However, the deletion of α_1 and α_2 significantly affected the secretion efficiency of Vip3Aa. Thus, α_1 and α_2 may serve as sorting signals of vesicular secretory proteins.

2.5. The Signal Region of Vip3Aa Can Direct Other Proteins into Vesicles

When the *chiB* gene without signal peptide sequence was expressed in Bt BMB171, ChiB protein accumulated in the cytoplasm instead of appearing in the culture supernatant. However, when replacing the signal peptide sequence with Vip3A 3 possible signal regions, N₁ (N-terminal 77 amino acids including α_1 and α_2), N₂ (N₁ without α_2) and N₃ (N₁ without α_1), (Figure 5a) ChiB could be detected in the supernatant when α_1 exists (Figure 5b). Thus, α_1 appears to play an essential role in protein secretion. Moreover, ChiB was detected in vesicles collected from the supernatant (Figure 5c), suggesting that MVs can transport other secreted proteins if appropriate signaling regions are available.

Contrary to Vip3A, the α_2 -helix is not indispensable for guiding the secretion of ChiB. The N-terminal 39 amino acid sequence of Vip3Aa, which includes α_1 and the N-terminal 22 amino acids in front of α_1 (Figure 5c), is enough for ChiB's MV transport. Consequently, we refer to it as the signal region responsible for MV secretion. In addition, we found when we removed the N-terminal 22 amino acids in front of α_1 , ChiB accumulated in the intracellular. This suggests that N-terminal 22 amino acids or α_1 is indispensable (Figure 5d).

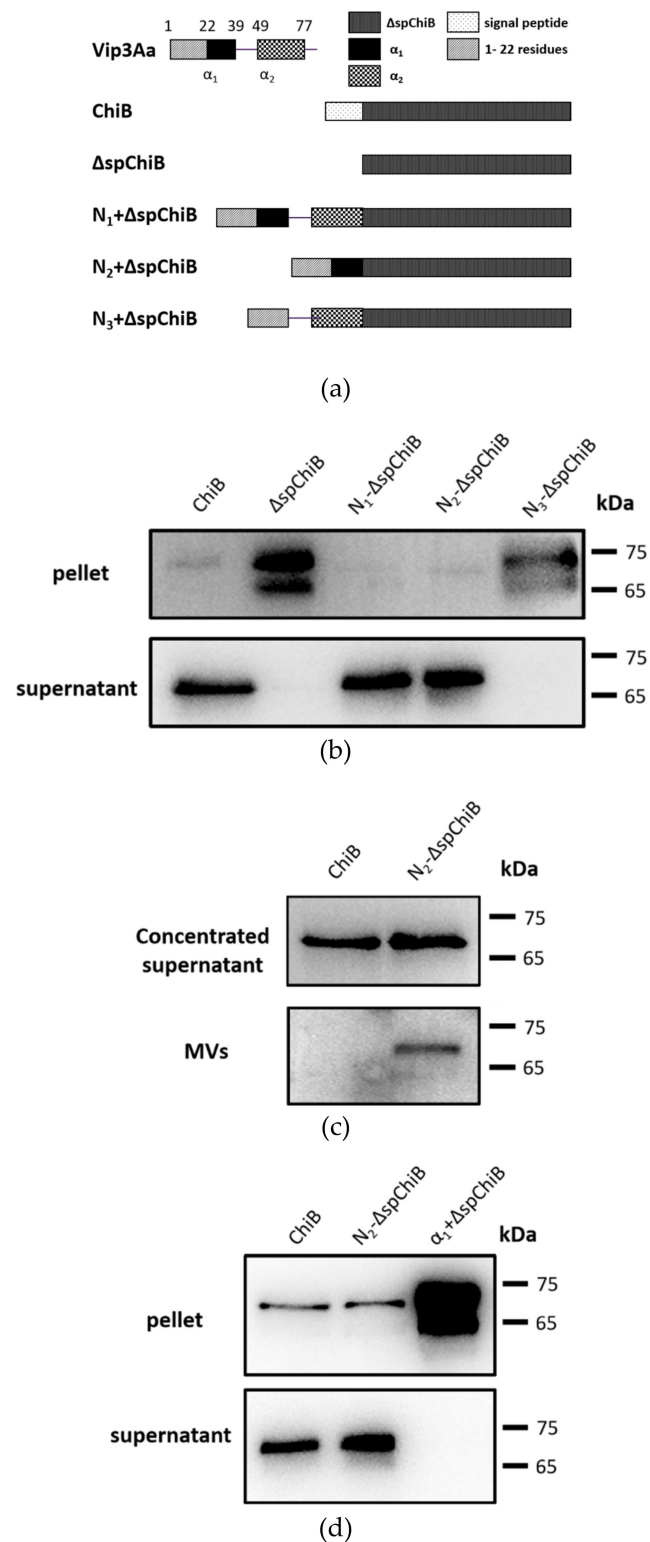


Figure 5. Identification of the signal regions for MV secretion. (a) Replacing the *chiB* signal peptide sequence with Vip3A possible signal regions. (b) Western blot analysis of ChiB, Δ spChiB, N_1 - Δ spChiB, N_2 - Δ spChiB and N_3 - Δ spChiB expressed in BMB171. Samples were collected at 12 h. (c) Concentrated supernatant (upper panel) and MVs (lower panel) purified from the culture media of BMB171/ChiB and BMB171/ N_2 - Δ spChiB were analyzed by Western blotting. (d) Western blot analysis of ChiB expressed in BMB171/ChiB, BMB171/ N_2 - Δ spChiB and BMB171/ α_1 + ChiB. Samples were collected at 12 h.

3. Discussion

In 1996, Estruch et al. first discovered Vip3A and noticed it is secreted without N-terminal processing [20]. They suggested that a non-classical secretion pathway secretes Vip3Aa. After that, few researchers explored the secretion mode of Vip3A.

At least ten secretion systems (the Sec system, the TAT system, secretion systems I–VII, and outer membrane vesicles) have been identified in Gram-negative bacteria [24,25]. By comparison, much fewer systems are present in Gram-positive bacteria [26]. Type V (T5SS) and type VI (T6SS) secretion systems with antibacterial effects are restricted to Gram-negative bacteria. Type VII secretion systems (T7SSs) in *Mycobacterium tuberculosis* secrete virulence factors belonging to the WXG100 family. In addition, T7SS of Gram-positive bacteria may secrete a class of putative antibacterial toxins [27].

Using the online software signalp-6.0, we found that the N-terminal sequence of Vip3A has no typical Sec and TAT signal peptides features. Moreover, Sec pathway improvement does not facilitate Vip3A secretion in this study. Thus, our results indicated that these two well-documented secretion pathways do not secrete Vip3Aa.

Since 1965, membrane vesicles (MVs) produced by the outer membrane of Gram-negative bacteria were first detected [27], and membrane vesicles have been observed in many bacteria. Vesicles have also been isolated and purified from Gram-positive bacteria over the past two decades [23,26], and some scholars term them CMVs [28], which are derived from cytoplasmic membranes. Although some evidence indicates that vesicles from Gram-negative and Gram-positive share a lot of properties and capabilities [29], vesicle secretion in Gram-positive bacteria is less studied. It seems that it has never been explored as a secretory pathway.

In this study, *B. thuringiensis* MVs were detected in size between 40 and 200 nm, expanding the horizon for MVs in Gram-positive bacteria. More importantly, Vip3A was confirmed to be transported by MVs. To our knowledge, it is the first time to reveal the secretion pathway of Vip3A.

In addition, Wang et al. [30] reported that Vip3Aa secretion is nutrient-dependent. When grown in a sporulation medium, Vip3Aa were not secreted to the culture solution but were retained in the mother cell compartment. However, when the strains were cultured in a rich medium, a fraction of Vip3Aa was secreted. Similarly, it was found that the MV yield of *Pseudomonas putida* KT2440 in LB media was three-fold increased than that of the minimal medium [31]. Given that, we hypothesized that oligonutrition blocks the vesicle formation and further impedes the secretion of Vip3A [32]. Thus, the optimal culture condition needs to be explored to improve MV secretion efficiency.

High concentrations of Vip3A are prone to form tetramers. An essential characteristic of MVs is the enrichment of specific protein and lipid cargo [33]. In this secretion pathway, the presence of vesicles may contribute to the formation of the Vip3A tetramer structure. Vesicles may provide a space for Vip3A, where its monomers can aggregate with each other and avoid being cleaved by proteases due to the protection of the membrane. As with Vip3A, inactive ClyA monomers in *E.coli* are packed into the OMVs and polymerized into a potent toxin in OMVs [34].

The production of extracellular vesicles in bacteria is a well-documented process, but the cargo selection mechanism of MVs is poorly understood [35]. A conserved, negatively charged amino acid motif known as the lipoprotein export signal (LES) domain is required for surface exposure of vesicles lipoproteins in *Bacteroidetes*. The LES domain is the first identified vesicles protein-sorting signal [36].

After determining that MVs secrete Vip3A, we tried to identify the signal region responsible for vesicle transport. For Vip3A, it still be secreted when the α_1 is removed. One possible explanation is that there are five α helices in Vip3A domain I. When α_1 is missing, the latter helices may play a complementary role. For ChiB without its signal peptide, our results showed that the N-terminal 39 amino acid sequence of Vip3Aa could efficiently guide it to the culture medium. Consequently, we proposed that the Vip3Aa

N-terminal sequence with conservative secondary structure is the signal region for MV sorting, which needs further exploration.

Bacillus is an attractive host for producing heterologous proteins, capable of secreting functional extracellular proteins directly to the culture medium [37]. However, some heterologous proteins are degraded by the host proteases during the secretory process, or traditional signal peptides cannot effectively transport these proteins to the medium. Using typical signal peptides to lead Vip3A secretion, we found that the secretion efficiency and protein stability of Vip3A decreased. Instead, when the Vip3A signal region was used to guide the secretion of ChiB, the transport efficiency was increased, accompanying the improvement of protein stability relative to its signal peptide. This may be because the MV membrane structure protects the packed proteins, which confers MV secretion advantages compared with traditional secretion systems.

MVs have potential in medicine, biology, and nanotechnology, such as employed in nanotechnology, delivering antibiotics or anticancer drugs, and killing bacteria [38,39]. They can also be developed into effective vaccines [40,41], and vesicle immunization effectively protects mice from *B. anthracis* [23]. *B. thuringiensis* BMB171 is nonpathogenic and has little impact on human and animal safety. Heterologously expressing toxin in BMB171 using the MV signal region, biomolecules can be delivered and brought together in MVs. Compared with *B. anthracis* MVs, BMB171 MVs undoubtedly have better potential as a vaccine. In addition, they can certainly be used for DNA and RNA transfer as well [42].

4. Conclusions

Overall, our results unveiled that the MV pathway secretes Vip3A. Its N-terminal 39 amino acid sequence, including α_1 , is the transport signal region, which can also lead other proteins to be secreted by vesicles. Our results will contribute to increasing the secretory efficiency of Vip3A. Likewise, it provides a new idea for the efficient transport of other proteins and has bright application prospects in the medicine and pharmaceutical field.

5. Materials and Methods

5.1. Bacterial Strains and Plasmids

The shuttle vector pHT1K was used for constructing protein expression vectors, and pRB1028 was applied for constructing the gene-integrating expression vectors in this study. The bacterial strains and plasmids used in this study are listed in Table 1.

Table 1. Bacterial strains and plasmids used in this study.

Strains and Plasmids	Relevant Properties	Source of Reference
<i>Escherichia coli</i>		
DH5 α	F- ϕ 80 <i>lac</i> Z Δ M15 Δ (<i>lacZYA-arg F</i>) U169 <i>endA1 recA1 hsdR17</i> (r_k^- , m_k^+) <i>supE44</i> λ - <i>thi-1 gyrA96 relA1phoA</i> ; host strain for plasmid construction	Stored in lab
<i>Bacillus thuringiensis</i>		
BMB171	An acrySTALLIFEROUS mutant strain; high transformation frequency	[43]
BMB171-Sec	<i>secYEG</i> integrate into BMB171 genome, overexpression of <i>secYEG</i> in BMB171	This study
BMB171/pHT- <i>vip3Aa</i>	BMB171 harboring pHT- <i>vip3Aa</i>	This study
BMB171/pPCsp <i>vip3</i>	BMB171 harboring pPCsp <i>vip3</i>	This study
BMB171-Sec/pHT- <i>vip3Aa</i>	BMB171-Sec harboring pHT- <i>vip3Aa</i>	This study
BMB171/pHT- <i>mbp</i>	BMB171 harboring pHT- <i>mbp</i>	This study
BMB171-Sec/pHT- <i>mbp</i>	BMB171-Sec harboring pHT- <i>mbp</i>	This study
BMB171/pP $\Delta\alpha_1$ <i>vip</i>	BMB171 harboring pP $\Delta\alpha_1$ <i>vip</i>	This study
BMB171/pP $\Delta\alpha_2$ <i>vip</i>	BMB171 harboring pP $\Delta\alpha_2$ <i>vip</i>	This study
BMB171/pP $\Delta\alpha_3$ <i>vip</i>	BMB171 harboring pP $\Delta\alpha_3$ <i>vip</i>	This study
BMB171/pP $\Delta\alpha_4$ <i>vip</i>	BMB171 harboring pP $\Delta\alpha_4$ <i>vip</i>	This study
BMB171/pHT- <i>chiB</i>	BMB171 harboring pHT- <i>chiB</i>	This study

Table 1. Cont.

Strains and Plasmids	Relevant Properties	Source of Reference
BMB171/pHT- Δ spchiB	BMB171 harboring pHT- Δ spchiB	This study
BMB171/pPN ₁ Δ spchiB	BMB171 harboring pPN ₁ Δ spchiB	This study
BMB171/pPN ₂ Δ spchiB	BMB171 harboring pPN ₂ Δ spchiB	This study
BMB171/pPN ₃ Δ spchiB	BMB171 harboring pPN ₃ Δ spchiB	This study
BMB171/pP α ₁ V Δ spchiB	BMB171 harboring pP α ₁ V Δ spchiB	This study
<i>Plasmids</i>		
pHT1k	<i>E. coli</i> and <i>B. thuringiensis</i> shuttle vector; Amp ^R , Erm ^R	[44]
pHT-vip3Aa	pHT1K + Promotor- <i>Prsi</i> + vip3Aa	This study
pPCspvip3	pHT1K + Promotor- <i>Prsi</i> + signal peptide of ChiB + vip3Aa	This study
pHT- <i>mbp</i>	pHT1K + Promotor- <i>Prsi</i> + <i>mbp</i>	This study
pP Δ α ₁ vip	pHT1K + Promotor- <i>Prsi</i> + Δ α ₁ vip3Aa	This study
pP Δ α ₂ vip	pHT1K + Promotor- <i>Prsi</i> + Δ α ₂ vip3Aa	This study
pP Δ α ₃ vip	pHT1K + Promotor- <i>Prsi</i> + Δ α ₃ vip3Aa	This study
pP Δ α ₄ vip	pHT1K + Promotor- <i>Prsi</i> + Δ α ₄ vip3Aa	This study
pHT- <i>chiB</i>	pHT1K + Promotor- <i>Prsi</i> + <i>chiB</i>	This study
pHT- Δ spchiB	pHT1K + Promotor- <i>Prsi</i> + Δ spchiB	This study
pPN ₁ Δ spchiB	pHT1K + Promotor- <i>Prsi</i> + N ₁ (N-terminal 77 amino acids of Vip3Aa including α 1 and α 2) + Δ spchiB	This study
pPN ₂ Δ spchiB	pHT1K + Promotor- <i>Prsi</i> + N ₂ (N-terminal 39 amino acids of Vip3Aa including α 1) + Δ spchiB	This study
pPN ₃ Δ spchiB	pHT1K + Promotor- <i>Prsi</i> + N ₃ (N-terminal 22 amino acids and α 2 of Vip3Aa) + Δ spchiB	This study
pP α ₁ V Δ spchiB	pHT1K + Promotor- <i>Prsi</i> + α 1 of Vip3Aa + Δ spchiB	This study
pRB1028	<i>B. thuringiensis</i> knockout vector; spc ^R	Stored in lab
pRB- <i>secYEG</i>	pRB1028- <i>secYEG</i> (U + <i>secYEG</i> + D); to overexpress <i>secYEG</i>	This study

AmpR, ampicillin resistance; EmrR, erythromycin resistance; SpcR, spectinomycin resistance.

5.2. Media and Cultural Conditions

Recombinant *E. coli* strains were cultivated at 37 °C in Luria–Bertani (LB) broth (10 g/L NaCl, 10 g/L tryptone, 5 g/L yeast extract, pH 7.0) with shaking at 200 rpm. *B. thuringiensis* were incubated at 28 °C with shaking at 200 rpm. The corresponding titer of antibiotic (50 µg/mL ampicillin, 50 µg/mL erythromycin or 20 µg/mL kanamycin) was added into the medium if necessary.

5.3. Gene Integration in *B. thuringiensis*

The genes *secY*, *secE*, *secG* mediated by *Prsi* promoter were integrated into the genome of *B. thuringiensis* BMB171 to over express *secYEG* according to previously reported method [20,21]. The construction procedure of BMB171-Sec was described briefly as follows. First, the upstream (U), *secY*, *secE*, *secG* and downstream (D) were amplified, respectively, using PCR with *B. thuringiensis* BMB171 genomic DNA as the template, fused by splicing overlap extension (SOE)-PCR using the primers U-F/D-R. The fused fragments were inserted into the pRB1028 at the restriction sites *HandIII* and *BamHI* by using the pEASY[®]-Basic Seamless Cloning and Assembly Kit (TransGen Biotech, Beijing, China). pRB-*secYEG* was constructed successfully after DNA sequencing and was electro-transferred into *B. thuringiensis* BMB171. The positive transformants were cultivated in the 5 mL LB liquid medium with 300 µg/mL spectinomycin at 28 °C, 200 r/min for 6–12h, and subcultured for 5–10 generation. Bacteria were streaked onto Spc300-plates and left overnight at 28 °C, and single colonies were picked and cultured in LB liquid for PCR analysis to screen the single-crossover colonies. Following clone examination by bacterial fluid PCR, the positive clones were subcultured in LB liquid medium without spc300 at 37 °C for 8 h, and subcultured for 5–10 generation. Bacteria were streaked onto LB plates and left overnight at 28 °C, and each single colony was inoculated onto LB plate with or without Spc300. The double crossover-colonies can only grow on the LB plate. After DNA sequencing, *secYEG* overexpressed strain (*B. thuringiensis* BMB171-Sec) was constructed successfully.

5.4. Construction of the Protein Expression Vector

The Vip3Aa, MBP, ChiB expression vector used in this study was constructed according to the following method. In previous work from our laboratory, we found *Prsi* is a strong constitutive promoter, it was amplified from Bti75. The DNA of *vip3Aa*, $\Delta\alpha_1vip$, $\Delta\alpha_2vip$, $\Delta\alpha_3vip$, $\Delta\alpha_4vip$, N_1 , N_2 and N_3 was amplified from the Vip3Aa11 gene (Genbank accession No. AY489126.1). The DNA of *chiB* and $\Delta spchiB$ was amplified from the plasmid BMB171/*chiB* stored in lab. The gene *mpb* coding for MBP was amplified from the genome DNA of DH5 α . The DNA fragments were purified, respectively, fused by SOE-PCR, and inserted into the expression vector pHT1K at the restriction sites *NcoI* and *KpnI*. All plasmids were constructed by using the pEASY[®]-Basic Seamless Cloning and Assembly Kit (TransGen Biotech, Beijing, China), and the reactions system was transformed into *E. coli* DH5 α . After plasmids sequencing, the recombinant plasmids were electro-transferred into the *B. thuringiensis* and verified by diagnostic PCR. All plasmids constructed in this study are listed in Table 1. All the primers used in this study are listed in Supplementary Table S1.

5.5. RNA Extraction and qRT-PCR

The total RNA was extracted by using the TRIzol[®] Reagent (Invitrogen, Waltham, MA, USA) and then quantified using NanoDrop technology (Thermo Scientific, Santa Clara, CA, USA). cDNA was synthesized using a PrimeScript[™] RTreagent Kit with gDNA Eraser (Takara, Japan) according to the manufacturer's instructions. The cDNA was then used as the template for quantitative real-time PCR (qPCR). Quantitative real-time reverse transcription PCR (qRT-PCR) was performed using TB Green[®] Premix Ex Taq[™] II (Takara) and the PCR products were detected with the StepOnePlusReal-Time PCR System (Applied Biosystems, Foster City, CA, USA). The relative expression level of each gene was calculated according to the 2-11CT method using 16S rRNA from *B. thuringiensis* BMB171 as an internal control.

5.6. Western Blotting

Pellets were resuspended in lysis buffer, cells were disrupted by sonication and the lysate was clarified by centrifugation. Culture supernatants and lysates were added into 5x Laemmli sample buffer and boiled for 10 min, separated on a 12% SDS/PAGE, and transferred to nitrocellulose membrane. Membrane was blocked for 2 h with non-fat milk and incubated for 1 h with polyclonal antibodies. After washing five times in TBST, the membrane was incubated with secondary antibodies for 1 h and five times washing. Protein bands were visualized using an enhanced chemiluminescence.

5.7. Purification of MVs

MVs were purified from *B. thuringiensis* supernatants with some modified purification methods of one-step sucrose cushion ultracentrifugation (SUC) method [45]. Briefly, overnight activated strains were inoculated to 1L of LB to bring its OD600 to 0.1, and were grown for 12 h at 28 °C with gentle shaking (150 rpm). After the cells were pelleted at 10,000 $\times g$ for 20 min, the supernatant was filtered through a 0.45 mm vacuum filter, and the filtrate was concentrated to 70 mL by ultrafiltration with 100 kDa Amicon Ultra centrifugal filter tube (Millipore, Burlington, MA, USA). The concentrated solution was again filtered through a 0.22 mm vacuum filter. The filtrate was loaded over 4 mL of 30% sucrose solution (in 1 \times PBS) and centrifuged at 150,000 $\times g$ for 1.5 h at 4 °C. The pellets were resuspended in PBS and washed by ultracentrifugation at 150,000 $\times g$ for 1.5 h at 4 °C. MVs were resuspended in 200 μ L 1 \times PBS and stored at -80 °C until use. DLS measurement was performed to measure the diameter of MVs using a DLS analyzer.

5.8. TEM Analysis

MV suspension was mixed with an equal volume of 4% PFA. Sample was placed in Formvar-carbon-coated copper grids and allowed to adsorb for 20 min in dry environment. Grids are washed with PBS and transferred to a 50- μ L drop of 1% glutaraldehyde for 2 min.

Then, transfer to a 100- μ L drop of distilled water for 2 min. Repeat seven times. Transfer grids to a 20- μ L drop of 2% uranium acetate solution for 2 min. After this, air dry the grid and observe it under the transmission electron microscope (TEM) (HT7700, Tokyo, Japan).

5.9. IEM Analysis

MV suspension was mixed with an equal volume of 4% PFA. Sample was placed in Formvar-carbon-coated copper grids and allowed to adsorb for 20 min in dry environment. Transfer grid to PBS and wash twice for 3 min. Permeabilization was performed with 0.1% sapon for 30 min. Transfer grid to PBS/50 mM glycine for 3 min. Transfer grids to a drop of 5% BSA for 10 min to blocking. Transfer the grid to a drop of diluted first antibody and incubate 30 min. Transfer grids to the appropriate washing buffer and wash 3 min. Repeat transfers to drops of washing buffer for a total of six washes. Transfer grids to a drop of diluted 6-nm colloidal gold-labeled secondary antibody, and incubate 30 min. Transfer grids to drops of PBS/0.5% BSA for a total of six washes. Transfer grids to drops of PBS and wash 2 min for 6 times. Transfer grids to 50- μ L drops of 1% glutaraldehyde for 2 min. Then, transfer to a 100- μ L drop of distilled water for 2 min. Repeat seven times. Transfer grids to a 20- μ L drop of 2% uranium acetate solution for 2 min. After this, air dry the grid and observe it under the electron microscope.

Supplementary Materials: The following supporting information can be downloaded at: <https://www.mdpi.com/article/10.3390/toxins14070480/s1>, Table S1: Oligonucleotides used in this study.

Author Contributions: Data curation, Y.Z.; funding acquisition, J.C.; investigation, Y.Z., X.L., H.T., B.A. and B.Y.; methodology, Y.Z. and X.L.; project administration, J.C.; supervision, J.C.; writing—original draft, Y.Z.; writing—review and editing, J.C. All authors have read and agreed to the published version of the manuscript.

Funding: This study was research was funded by the National Key R&D Program of China (No. 2017YFD0200400), and the National Natural Science Foundation of China (No. 31371979).

Institutional Review Board Statement: Not applicable.

Informed Consent Statement: Not applicable.

Conflicts of Interest: The authors declare no conflict of interest.

References

1. Liu, J.G.; Yang, A.Z.; Shen, X.H.; Hua, B.G.; Shi, G.L. Specific binding of activated Vip3Aa10 to *Helicoverpa armigera* brush border membrane vesicles results in pore formation. *J. Invertebr. Pathol.* **2011**, *108*, 92–97. [CrossRef] [PubMed]
2. Chakrabarty, S.; Jin, M.; Wu, C.; Chakraborty, P.; Xiao, Y. Bacillus thuringiensis vegetative insecticidal protein family Vip3A and mode of action against pest Lepidoptera. *Pest. Manag. Sci.* **2020**, *76*, 1612–1617. [CrossRef] [PubMed]
3. Chakroun, M.; Bel, Y.; Caccia, S.; Abdelkefi-Mesrati, L.; Escriche, B.; Ferre, J. Susceptibility of *Spodoptera frugiperda* and *S. exigua* to *Bacillus thuringiensis* Vip3Aa insecticidal protein. *J. Invertebr. Pathol.* **2012**, *110*, 334–339. [CrossRef] [PubMed]
4. Gupta, M.; Kumar, H.; Kaur, S. Vegetative Insecticidal Protein (Vip): A Potential Contender From *Bacillus thuringiensis* for Efficient Management of Various Detrimental Agricultural Pests. *Front. Microbiol.* **2021**, *12*, 659736. [CrossRef]
5. Yang, J.; Quan, Y.; Sivaprasath, P.; Shabbir, M.Z.; Wang, Z.; Ferre, J.; He, K. Insecticidal Activity and Synergistic Combinations of Ten Different Bt Toxins against *Mythimna separata* (Walker). *Toxins* **2018**, *10*, 454. [CrossRef]
6. Wang, Z.; Fang, L.; Zhou, Z.; Pacheco, S.; Gomez, I.; Song, F.; Soberon, M.; Zhang, J.; Bravo, A. Specific binding between *Bacillus thuringiensis* Cry9Aa and Vip3Aa toxins synergizes their toxicity against Asiatic rice borer (*Chilo suppressalis*). *J. Biol. Chem.* **2018**, *293*, 11447–11458. [CrossRef]
7. Tabashnik, B.E.; Liesner, L.R.; Ellsworth, P.C.; Unnithan, G.C.; Fabricck, J.A.; Naranjo, S.E.; Li, X.; Dennehy, T.J.; Antilla, L.; Staten, R.T.; et al. Transgenic cotton and sterile insect releases synergize eradication of pink bollworm a century after it invaded the United States. *Proc. Natl. Acad. Sci. USA* **2021**, *118*, e2019115118. [CrossRef]
8. Syed, T.; Askari, M.; Meng, Z.; Li, Y.; Abid, M.A.; Wei, Y.; Guo, S.; Liang, C.; Zhang, R. Current Insights on Vegetative Insecticidal Proteins (Vip) as Next Generation Pest Killers. *Toxins* **2020**, *12*, 522. [CrossRef]
9. Jiang, K.; Zhang, Y.; Chen, Z.; Wu, D.; Cai, J.; Gao, X. Structural and Functional Insights into the C-terminal Fragment of Insecticidal Vip3A Toxin of *Bacillus thuringiensis*. *Toxins* **2020**, *12*, 438. [CrossRef]
10. Nunez-Ramirez, R.; Huesa, J.; Bel, Y.; Ferre, J.; Casino, P.; Arias-Palomo, E. Molecular architecture and activation of the insecticidal protein Vip3Aa from *Bacillus thuringiensis*. *Nat. Commun.* **2020**, *11*, 3974. [CrossRef]

11. Byrne, M.J.; Iadanza, M.G.; Perez, M.A.; Maskell, D.P.; George, R.M.; Hesketh, E.L.; Beales, P.A.; Zack, M.D.; Berry, C.; Thompson, R.F. Cryo-EM structures of an insecticidal Bt toxin reveal its mechanism of action on the membrane. *Nat. Commun.* **2021**, *12*, 2791. [[CrossRef](#)] [[PubMed](#)]
12. Singh, G.; Sachdev, B.; Sharma, N.; Seth, R.; Bhatnagar, R.K. Interaction of *Bacillus thuringiensis* vegetative insecticidal protein with ribosomal S2 protein triggers larvicidal activity in *Spodoptera frugiperda*. *Appl. Environ. Microbiol.* **2010**, *76*, 7202–7209. [[CrossRef](#)] [[PubMed](#)]
13. Jiang, K.; Hou, X.Y.; Tan, T.T.; Cao, Z.L.; Mei, S.Q.; Yan, B.; Chang, J.; Han, L.; Zhao, D.; Cai, J. Scavenger receptor-C acts as a receptor for *Bacillus thuringiensis* vegetative insecticidal protein Vip3Aa and mediates the internalization of Vip3Aa via endocytosis. *PLoS Pathog.* **2018**, *14*, e1007347. [[CrossRef](#)]
14. Jiang, K.; Hou, X.; Han, L.; Tan, T.; Cao, Z.; Cai, J. Fibroblast Growth Factor Receptor, a Novel Receptor for Vegetative Insecticidal Protein Vip3Aa. *Toxins* **2018**, *10*, 546. [[CrossRef](#)] [[PubMed](#)]
15. Osman, G.H.; Soltane, R.; Saleh, I.; Abulreesh, H.H.; Gazi, K.S.; Arif, I.A.; Ramadan, A.M.; Alameldin, H.F.; Osman, Y.A.; Idriss, M. Isolation, characterization, cloning and bioinformatics analysis of a novel receptor from black cut worm (*Agrotis ipsilon*) of *Bacillus thuringiensis* vip 3Aa toxins. *Saudi J. Biol. Sci.* **2019**, *26*, 1078–1083. [[CrossRef](#)] [[PubMed](#)]
16. An, B.; Zhang, Y.; Li, X.; Hou, X.; Yan, B.; Cai, J. PHB2 affects the virulence of Vip3Aa to Sf9 cells through internalization and mitochondrial stability. *Virulence* **2022**, *13*, 684–697. [[CrossRef](#)] [[PubMed](#)]
17. Hernandez-Martinez, P.; Gomis-Cebolla, J.; Ferre, J.; Escrache, B. Changes in gene expression and apoptotic response in *Spodoptera exigua* larvae exposed to sublethal concentrations of Vip3 insecticidal proteins. *Sci. Rep.* **2017**, *7*, 16245. [[CrossRef](#)]
18. Jiang, K.; Mei, S.Q.; Wang, T.T.; Pan, J.H.; Chen, Y.H.; Cai, J. Vip3Aa induces apoptosis in cultured *Spodoptera frugiperda* (Sf9) cells. *Toxicon* **2016**, *120*, 49–56. [[CrossRef](#)]
19. Hou, X.; Han, L.; An, B.; Zhang, Y.; Cao, Z.; Zhan, Y.; Cai, X.; Yan, B.; Cai, J. Mitochondria and Lysosomes Participate in Vip3Aa-Induced *Spodoptera frugiperda* Sf9 Cell Apoptosis. *Toxins* **2020**, *12*, 116. [[CrossRef](#)]
20. Estruch, J.J.; Warren, G.W.; Mullins, M.A.; Nye, G.J.; Craig, J.A.; Koziel, M.G. Vip3A, a novel *Bacillus thuringiensis* vegetative insecticidal protein with a wide spectrum of activities against lepidopteran insects. *Proc. Natl. Acad. Sci. USA* **1996**, *93*, 5389–5394. [[CrossRef](#)]
21. Shao, H.; Im, H.; Castro, C.M.; Breakefield, X.; Weissleder, R.; Lee, H. New Technologies for Analysis of Extracellular Vesicles. *Chem. Rev.* **2018**, *118*, 1917–1950. [[CrossRef](#)] [[PubMed](#)]
22. Zack, M.D.; Sopko, M.S.; Frey, M.L.; Wang, X.; Tan, S.Y.; Arruda, J.M.; Letherer, T.T.; Narva, K.E. Functional characterization of Vip3Ab1 and Vip3Bc1: Two novel insecticidal proteins with differential activity against lepidopteran pests. *Sci. Rep.* **2017**, *7*, 11112. [[CrossRef](#)] [[PubMed](#)]
23. Rivera, J.; Cordero, R.J.; Nakouzi, A.S.; Frases, S.; Nicola, A.; Casadevall, A. *Bacillus anthracis* produces membrane-derived vesicles containing biologically active toxins. *Proc. Natl. Acad. Sci. USA* **2010**, *107*, 19002–19007. [[CrossRef](#)] [[PubMed](#)]
24. Mekasha, S.; Linke, D. Secretion Systems in Gram-Negative Bacterial Fish Pathogens. *Front. Microbiol.* **2021**, *12*, 782673. [[CrossRef](#)] [[PubMed](#)]
25. Gorasia, D.G.; Veith, P.D.; Reynolds, E.C. The Type IX Secretion System: Advances in Structure, Function and Organisation. *Microorganisms* **2020**, *8*, 1173. [[CrossRef](#)]
26. Zhang, J.; Pan, Z.Z.; Xu, L.; Liu, B.; Chen, Z.; Li, J.; Niu, L.Y.; Zhu, Y.J.; Chen, Q.X. Proteolytic activation of *Bacillus thuringiensis* Vip3Aa protein by *Spodoptera exigua* midgut protease. *Int. J. Biol. Macromol.* **2018**, *107*, 1220–1226. [[CrossRef](#)]
27. Lee, E.Y.; Choi, D.Y.; Kim, D.K.; Kim, J.W.; Park, J.O.; Kim, S.; Kim, S.H.; Desiderio, D.M.; Kim, Y.K.; Kim, K.P.; et al. Gram-positive bacteria produce membrane vesicles: Proteomics-based characterization of *Staphylococcus aureus*-derived membrane vesicles. *Proteomics* **2009**, *9*, 5425–5436. [[CrossRef](#)]
28. Bishop, D.G.; Work, E. An extracellular glycolipid produced by *Escherichia coli* grown under lysine-limiting conditions. *Biochem. J.* **1965**, *96*, 567–576. [[CrossRef](#)]
29. Toyofuku, M.; Nomura, N.; Eberl, L. Types and origins of bacterial membrane vesicles. *Nat. Rev. Microbiol.* **2019**, *17*, 13–24. [[CrossRef](#)]
30. Wang, Z.; Gan, C.; Wang, J.; Bravo, A.; Soberon, M.; Yang, Q.; Zhang, J. Nutrient conditions determine the localization of *Bacillus thuringiensis* Vip3Aa protein in the mother cell compartment. *Microb. Biotechnol.* **2021**, *14*, 551–560. [[CrossRef](#)]
31. Choi, C.W.; Park, E.C.; Yun, S.H.; Lee, S.Y.; Lee, Y.G.; Hong, Y.; Park, K.R.; Kim, S.H.; Kim, G.H.; Kim, S.I. Proteomic characterization of the outer membrane vesicle of *Pseudomonas putida* KT2440. *J. Proteome Res.* **2014**, *13*, 4298–4309. [[CrossRef](#)] [[PubMed](#)]
32. Orench-Rivera, N.; Kuehn, M.J. Environmentally controlled bacterial vesicle-mediated export. *Cell. Microbiol.* **2016**, *18*, 1525–1536. [[CrossRef](#)] [[PubMed](#)]
33. Roier, S.; Zingl, F.G.; Cakar, F.; Schild, S. Bacterial outer membrane vesicle biogenesis: A new mechanism and its implications. *Microb. Cell* **2016**, *3*, 257–259. [[CrossRef](#)]
34. Roderer, D.; Glockshuber, R. Assembly mechanism of the alpha-pore-forming toxin cytolysin A from *Escherichia coli*. *Philos. Trans. R. Soc. Lond. B Biol. Sci.* **2017**, *372*, 20160211. [[CrossRef](#)]
35. Sartorio, M.G.; Pardue, E.J.; Feldman, M.F.; Haurat, M.F. Bacterial Outer Membrane Vesicles: From Discovery to Applications. *Annu. Rev. Microbiol.* **2021**, *75*, 609–630. [[CrossRef](#)]

36. Valguarnera, E.; Scott, N.E.; Azimzadeh, P.; Feldman, M.F. Surface Exposure and Packing of Lipoproteins into Outer Membrane Vesicles Are Coupled Processes in *Bacteroides*. *mSphere* **2018**, *3*, e00559-18. [[CrossRef](#)]
37. Pohl, S.; Harwood, C.R. Heterologous protein secretion by bacillus species from the cradle to the grave. *Adv. Appl. Microbiol.* **2010**, *73*, 1–25. [[CrossRef](#)] [[PubMed](#)]
38. Naskar, A.; Cho, H.; Lee, S.; Kim, K.S. Biomimetic Nanoparticles Coated with Bacterial Outer Membrane Vesicles as a New-Generation Platform for Biomedical Applications. *Pharmaceutics* **2021**, *13*, 1887. [[CrossRef](#)]
39. Li, M.; Zhou, H.; Yang, C.; Wu, Y.; Zhou, X.; Liu, H.; Wang, Y. Bacterial outer membrane vesicles as a platform for biomedical applications: An update. *J. Control. Release* **2020**, *323*, 253–268. [[CrossRef](#)]
40. Chen, L.; Valentine, J.L.; Huang, C.J.; Endicott, C.E.; Moeller, T.D.; Rasmussen, J.A.; Fletcher, J.R.; Boll, J.M.; Rosenthal, J.A.; Dobruchowska, J.; et al. Outer membrane vesicles displaying engineered glycotopes elicit protective antibodies. *Proc. Natl. Acad. Sci. USA* **2016**, *113*, E3609–E3618. [[CrossRef](#)]
41. Irene, C.; Fantappie, L.; Caproni, E.; Zerbini, F.; Anesi, A.; Tomasi, M.; Zanella, I.; Stupia, S.; Prete, S.; Valensin, S.; et al. Bacterial outer membrane vesicles engineered with lipidated antigens as a platform for *Staphylococcus aureus* vaccine. *Proc. Natl. Acad. Sci. USA* **2019**, *116*, 21780–21788. [[CrossRef](#)] [[PubMed](#)]
42. Lecrivain, A.L.; Beckmann, B.M. Bacterial RNA in extracellular vesicles: A new regulator of host-pathogen interactions? *Biochim. Biophys. Acta Gene Regul. Mech.* **2020**, *1863*, 194519. [[CrossRef](#)] [[PubMed](#)]
43. He, J.; Shao, X.; Zheng, H.; Li, M.; Wang, J.; Zhang, Q.; Li, L.; Liu, Z.; Sun, M.; Wang, S.; et al. Complete genome sequence of *Bacillus thuringiensis* mutant strain BMB171. *J. Bacteriol.* **2010**, *192*, 4074–4075. [[CrossRef](#)] [[PubMed](#)]
44. Zheng, C.; Ma, Y.; Wang, X.; Xie, Y.; Ali, M.K.; He, J. Functional analysis of the sporulation-specific diadenylate cyclase CdaS in *Bacillus thuringiensis*. *Front. Microbiol.* **2015**, *6*, 908. [[CrossRef](#)] [[PubMed](#)]
45. Gupta, S.; Rawat, S.; Arora, V.; Kottarath, S.K.; Dinda, A.K.; Vaishnav, P.K.; Nayak, B.; Mohanty, S. An improvised one-step sucrose cushion ultracentrifugation method for exosome isolation from culture supernatants of mesenchymal stem cells. *Stem Cell Res. Ther.* **2018**, *9*, 180. [[CrossRef](#)]